The Cockcroft Institute
of Accelerator Science and Technology

Cockcroft-12-24

RF AND SURFACE PROPERTIES OF BULK NIOBIUM AND NIOBIUM FILM SAMPLES

Tobias Junginger, CERN, Geneva, Switzerland and MPIK Heidelberg, Germany †
Rebecca Seviour, ESS - Scandinavia, Sweden and University of Huddersfield, UK
WolfgangWeingarten, CERN, Geneva, Switzerland
Carsten Welsch, Cockcroft Institute,Warrington and University of Liverpool, UK

RF AND SURFACE PROPERTIES OF BULK NIOBIUM AND NIOBIUM FILM SAMPLES

Tobias Junginger, CERN, Geneva, Switzerland and MPIK Heidelberg, Germany †
Rebecca Seviour, ESS - Scandinavia, Sweden and University of Huddersfield, United Kingdom
Wolfgang Weingarten, CERN, Geneva, Switzerland
Carsten Welsch, Cockcroft Institute, Warrington and University of Liverpool, United Kingdom

Abstract

At CERN a compact Quadrupole Resonator has been developed for the RF characterization of superconducting samples at different frequencies. In this contribution measurements on bulk niobium and niobium film on copper samples are presented. Surface resistance results are being correlated to surface analyses measurements carried out on the same samples.

INTRODUCTION

Currently, two different methods for manufacturing niobium RF cavities are used. They are either made of bulk niobium or a micrometer thin niobium film is deposited on the inner surface of a copper cavity. The latter approach has been successfully exploited at CERN for the Large Electron-Positron Collider (LEP) [1] and the Large Hadron Collider (LHC) [2]. It has several advantages compared to the bulk niobium technology. Copper is widely available and can be procured at lower cost. Its high thermal conductivity helps avoiding one of the possible failures of superconducting cavities, transition to the normal conducting state due to heating of a local defect, called quench. Usually niobium films are of lower purity than bulk niobium, resulting in lower losses from thermally activated normal conducting electrons, because the surface resistance of niobium is not at minimum for highest, but rather for intermediate purity material. Finally, thin film cavities are less sensitive to trapped flux from the earth's magnetic field and do therefore not require magnetic shielding. Despite all these advantages of niobium films, the bulk niobium technology was chosen for all future superconducting linear accelerator applications relying on a high accelerating gradient, such as the Continuous Electron Beam Accelerator Facility (CEBAF) upgrade, the European X-ray Free Electron Laser (XFEL) or the International Linear Collider (ILC). The reason is the lower increase of the surface resistance with accelerating gradient for bulk niobium cavities (Q-slope).

Recently it has been shown that interface tunnel exchange (ITE) acting between surface oxides and the adjacent superconducting material can give rise to losses on niobium film surfaces [3], while these losses are negligible for well prepared bulk niobium surfaces [4].

In this contribution it will be explained how one can distinguish between electric losses caused by ITE and magnetic losses by analyzing only a single curve surface resistance R_{S} vs. applied magnetic field B. The origin of losses caused by ITE is crack corrosion along grain boundaries [5]. Ultrasonic force microscopy is used to reveal the surface oxide structure of two samples, one where ITE losses are dominant and one where they are negligible.

* Work supported by the German Doctoral Students program of the Federal Ministry of Education and Research (BMBF)

† tobias.junginger@cern.ch

SURFACE RESISTANCE

Usually, when the surface resistance of superconducting cavities is investigated, the losses are assumed to be caused by the RF magnetic field B, since the contribution from the electric field E is negligible, even for normal conducting metals [6]. However for oxidized surfaces additional loss mechanisms need to be taken into account. Consider a niobium surface with oxides formed along its grain boundaries. When the RF field is raised the vertical electric field only penetrates the dielectric oxides but not the adjacent superconducting material. It becomes now energetically favorable for localized electrons to tunnel to the superconductor and when the field is lowered to return to the dielectric. This process occurs within a single RF cycle, yielding a surface resistance proportional to the RF frequency f [3].

For well prepared bulk niobium samples these losses are negligible. Here the field dependent surface resistance can be expressed by a quadratic factorization of the BCS surface resistance [4]. In general the total surface resistance of a superconductor at fields below the exponential increase at high fields (Q-drop) can be expressed by a sum of these two contributions plus an additional residual resistance R_{Res}:

$$R_{\mathrm{S}}(f,T,B,E) = R_{\mathrm{BCS}}(f,T)\left(1+\gamma B^2\right) + R_{\mathrm{S}}^{\mathrm{E}}(f,E) + R_{\mathrm{Res}}(f), \qquad (1)$$

with the electrical surface resistance $R_{\mathrm{S}}^{\mathrm{E}}$ caused by ITE

$$R_{\mathrm{S}}^{\mathrm{E}} = R_{\mathrm{S,sat}}^{\mathrm{E}}\left[\mathrm{e}^{-b/E} - \mathrm{e}^{-b/E^0}\right], \quad E \geq E^0, \qquad (2)$$

where the $R_{\mathrm{S,sat}}^{\mathrm{E}}$ is the surface resistance at saturation.

Figure 1 displays R_{S} of a micrometer thin niobium film sputtered on a copper substrate (top) and a reactor grade bulk niobium sample (bottom). Both samples were measured with the Quadrupole Resonator [7, 8] at 800 MHz and 4 K. From the shape of the curve one identify the dominant loss mechanism for each sample. The surface resistance of the thin film sample is clearly dominated by ITE. This can be seen, since the surface resistance increases only above a threshold field of about 7 mT and saturates at higher fields, where all localized states participate in the exchange. The

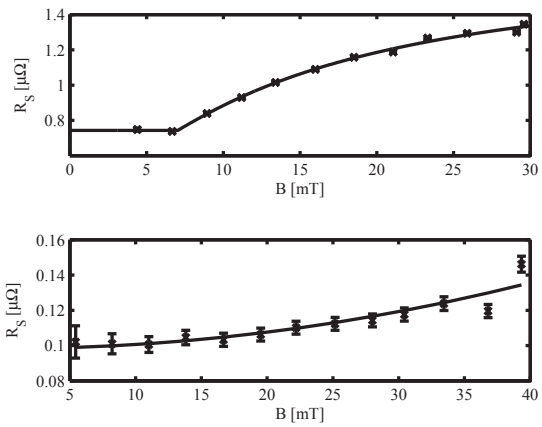

Figure 1: Surface resistance of a niobium thin film sample (top) and a bulk niobium sample (bottom) measured at 4 K and 800 MHz.

data can be fitted neglecting the non linear magnetic losses. The ITE mechanism is negligible for the bulk niobium sample. Here a quadratic factorization of the BCS losses is sufficient to obtain a good fit.

SURFACE ANALYSES

Correlating the different loss mechanisms dominant for the two samples to their surface properties is subject of this section. Above it has been shown that the field dependent surface resistance of the niobium film sample could be described by the interface tunnel exchange model. This model was not applicable to the data of the bulk niobium sample. Losses from interface tunnel exchange stem from oxides localized on the surface at distinct positions, for niobium films preferably along grain boundaries. The Young modulus of Nb_2O_5 was measured to be 125 GPa [9]. This is significantly higher than the value of niobium 105 GPa [10]. Therefore, mapping the elasticity of the two samples is interesting in order to find out whether there are differences in the oxygen distribution on the surface.

A method capable of this task is ultrasonic force microscopy (UFM) [11]. A UFM is built from an atomic force microscope by mounting the sample to a piezoelectric transducer [12]. By applying an alternating voltage to the transducer the sample is vertically vibrated at a frequency above the cantilever's primary resonance, increasing its effective spring constant due to inertia. The cantilever cannot follow the oscillation. This yields a constant feedback error signal, as long as tip and sample are in contact. Modulating the the oscillation in amplitude allows to derive the threshold where contact is lost, from a change in the feedback error signal. In practice this signal is transmitted to a lock-in amplifier as input, while the amplitude modulation frequency is used as the reference. The lock-in amplifier only gives a signal if the contact between sample and cantilever is lost. For a stiffer or less adhesive sample the threshold amplitude is lower and therefore the lock-in amplifier output larger. The convention for UFM images is to use a brighter color for a higher lock-in amplifier output corresponding to a stiffer or less adhesive sample [13]. Built upon an AFM, UFM also provides information about the topography and the lateral force. While the former gives an AFM image, the latter is used to distinguish between elastic and adhesive forces. In general the elastic forces are dominant [12] and for the forces applied in the nN range, plastic deformation was never observed, at least in the AFM resolution limit [13]. The structure of the bulk niobium sample appears more uniform compared to the niobium film, see Fig. 2 The softer (darker) regions of the latter are correlated to single niobium grains. Around the grains are harder (brighter) areas caused by oxidation preferably located along the grain boundaries. This explains why losses from interface tunnel exchange are the dominant mechanism of this sample and why these are negligible for the bulk niobium sample. The values obtained must be interpreted relatively with respect to each other. The test setup used does not enable to give a quantitative value of the Young modulus.

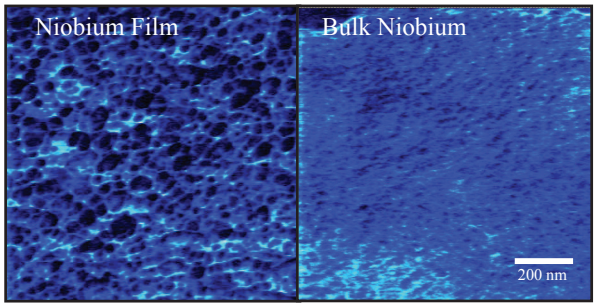

Figure 2: UFM images of a niobium film (left) and a bulk niobium sample (right). A dark (light) color indicate areas of low (high) elasticity. The lateral resolution of the pictures is 4 nm and the surface area displayed is 1x1 μm for each sample.

A tool enabling to provide information about the elemental composition is X-ray Photoelectron Spectroscopy (XPS). An XPS system uses an X-ray beam of usually 1-2 keV to irradiate the sample under investigation. The electrons knocked off from the sample have a kinetic energy

$$U_{\mathrm{kin}} = h\nu - U_{\mathrm{b}}, \tag{3}$$

where $h\nu$ is the incident photon energy and U_{b} the binding energy of the knocked-off electron. The photon energy is determined by the used XPS system, while the values of U_{b} can be taken from literature. For the analyses here the U_{b} values were taken from the NIST database [14]. This allows to derive the elemental composition from the measured spectrum.

Figure 3 shows XPS spectra for the niobium film and the bulk niobium sample. They were measured with a system at the University of Liverpool, using an Al K_α X-Ray

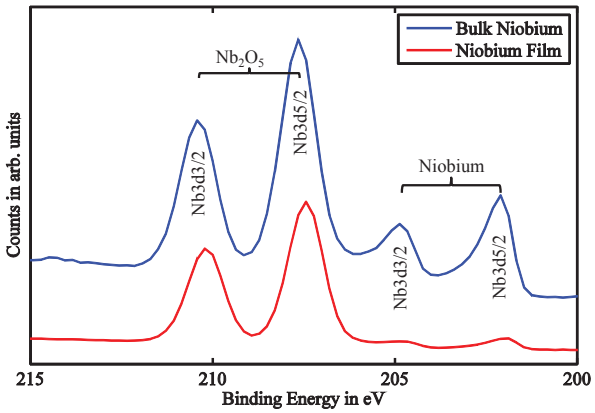

Figure 3: XPS spectra of the bulk niobium and the niobium film sample.

source with a photon energy hν=1486.6 eV [15]. This corresponds to an information depth of approximately 7 nm, covering the oxide and the oxide/metal interface.

A spectrum with an energy resolution of about 0.27 eV was obtained, see Fig. 3. The XPS signal-ratio between the niobium oxides and the metal is larger for the niobium film, confirming the stronger oxidation of this sample.

SUMMARY

Results from surface resistance, UFM and XPS measurements on a bulk niobium and a niobium film on a copper substrate sample have been presented. The surface resistance of the the two samples shows a different dependency on the applied field strength, indicating different loss mechanisms. UFM was used to reveal the distribution of oxides on the surfaces. XPS confirmed the presence of Nb_2O_5 and supports the interpretation of the ultrasonic force microscopy measurements and their correlation to the surface resistance results. The stronger Q-slope of sputter deposited niobium film- in comparison to bulk niobium cavities is correlated to the smaller grain size and higher oxygen content. This surface structure causes additional RF losses from interface tunnel exchange between the superconducting material and Nb_2O_5 formed along grain boundaries.

ACKNOWLEDGMENT

The authors would like to thank everybody who contributed to the refurbishment and operation of the Quadrupole Resonator. The work of S. Calatroni and S. Forel (preparation of samples) and the operators from the CERN cryogenics group is highly appreciated. We thank Ernst Haebel, now retired, for explaining to us the original idea and conception of the Quadrupole Resonator. UFM measurements were done in cooperation with Ilya Grishin (University of Lancaster), while XPS was performed by Paul Unsworth (University of Liverpool).

One of us (TJ) is also indebted to the German Ministry of Education and Research for being awarded a grant by the German Doctoral Program at CERN (Gentner - Program).

REFERENCES

[1] D. Boussard, Operational experience with the LEP2 SC cavity system, in *Proceedings of the 5th European Particle Accelerator Conference,*, pp. 187–191, 1996.

[2] D. Boussard, E. Chiaveri, E. Haebel, H. P. Kindermann, R. Losito, S. Marque, V. Rödel, and M. Stirbet, The LHC superconducting cavities, Technical report, 1999, LHC-Project-Report-301.

[3] T. Junginger, W. Weingarten, and C. Welsch, Losses in superconducting Niobium Films caused by Interface Tunnel Exchange, arXiv:1204.2166v1, submitted to Appl. Phys. Lett., 2012.

[4] T. Junginger, W. Weingarten, and C. Welsch, Review of RF Sample Test Equipment and Results, in *Proceedings of the 15th International Workshop on RF Superconductivity, Chicago, Ill., USA*, 2011.

[5] J. Halbritter, Residual Losses, High Electric and Magnetic RF Fields in Superconducting Cavities, in *Superconducting Materials for High Energy Colliders - Proceedings of the 38th Workshop of the INFN Eloisatron Project*, 1999.

[6] J. Halbritter, *Zeitschrift für Physik B* **31**, 19 (1978).

[7] E. Mahner, S. Calatroni, E. Chiaveri, E. Haebel, and J. M. Tessier, *Review of Scientific Instruments* **74**, 3390 (2003).

[8] T. Junginger, W. Weingarten, and C. Welsch, Extension of the Measurement Capabilities of the Quadrupole Resonator, arXiv:1204.1018v1 submitted to Rev. Scient. Instr., 2012.

[9] T. Chudoba, N. Schwarzer, and F. Richter, *Surface and Coatings Technology* **127**, 9 (2000).

[10] G. S. Brady, H. R. Clauser, and J. a. Vaccari, *Materials Handbook*, Mc Graw-Hill, 15th edition, 2002.

[11] K. Yamanaka, H. Ogisoa, and O. Kolosov, *Appl. Physics Letters* **64**, 178 (1994).

[12] A. Briggs and O. Kolosov, *Acoustic Microscopy*, Oxford University Press, 2nd edition, 2009.

[13] F. Dinelli, M. R. Castell, D. A. Ritchie, N. J. Mason, G. A. D. Briggs, and O. V. Kolosov, *Philosophical Magazine A* **80**, 2299 (2000).

[14] http://srdata.nist.gov/xps/; accessed 23.1.12.

[15] P. Unsworth, Supplier: VSW Company, Manchester. The instrument was designed to obtain an energy resolution of the order of 0.27eV. The X-ray source is Al K_α monochromatised with high flux output and a maximum operating power of 600W. The electron multi-detection system is comprised of a VSW HA150 hemispherical analyser used in fixed analyser transmission mode, private communication 24.01.2012.